

Cluster Bose Metals

Tao Ying,^{1,2,3} Marcello Dalmonte,^{4,5} Adriano Angelone,¹ Fabio Mezzacapo,¹ Peter Zoller,⁴ and Guido Pupillo¹

¹*icFRC, IPCMS (UMR 7504) and ISIS (UMR 7006),*

Université de Strasbourg and CNRS, 67000 Strasbourg, France

²*Institut für Theoretische Festkörperphysik, JARA-FIT and JARA-HPC,
RWTH Aachen University, 52056 Aachen, Germany*

³*Department of Physics, Harbin Institute of Technology, 150001 Harbin, China*

⁴*Institute for Theoretical Physics, University of Innsbruck,
and IQOQI of the Austrian Academy of Sciences, A-6020 Innsbruck, Austria*

⁵*International Center for Theoretical Physics, 34151 Trieste, Italy*

(Dated: December 9, 2024)

Quantum phases of matter are usually characterised by broken symmetries. Identifying physical mechanisms and microscopic Hamiltonians that elude this paradigm is one of the key present challenges in many-body physics. Here, we use quantum Monte-Carlo simulations to show that a Bose metal phase, breaking no symmetries, is realized in simple Hubbard models for bosonic particles on a square lattice complemented by soft-shoulder interactions. The Bose metal appears at strong coupling and is separated from a supersolid phase and a superfluid at weaker couplings. The enabling mechanism is provided by cluster formation in the corresponding classical tiling problem. The identification of the cluster mechanism paves the way to the realization of exotic quantum liquids in both natural and synthetic quantum matter that harbors cluster formation.

PACS numbers: 32.80.Ee, 67.80.K-, 05.30.Jp, 61.43.Fs

Many-body bosonic systems exist at low temperature in superfluid or insulating crystalline phases. These archetypical phases are described by finite values of order parameters, reflecting the broken symmetries of the ground state. A remarkable counterexample is provided by Bose metals describing conducting, yet non-superfluid bosons in two dimensions [1–4]. These phases have been suggested as a possible explanation for the strange metal behavior in high-temperature superconductors, and have been theoretically demonstrated in models supporting multi-particle ring-exchange-type interactions [4–6]. However, because of their inherently non-perturbative nature, identifying generic mechanisms and microscopic models that stabilize a Bose metal in realistic Hamiltonians with two-particle interactions has proven challenging.

Here, we show that a whole class of Bose-metal-type phases can be realised in Bose-Hubbard models on square lattices with soft-shoulder interactions, described by the following Hamiltonian

$$\mathcal{H} = -t \sum_{\langle i,j \rangle} (b_i^\dagger b_j + b_j^\dagger b_i) + (V/2) \sum_{i \neq j; r_{ij} \leq r_c} n_i n_j. \quad (1)$$

Here, b_i (b_i^\dagger) are hard-core bosonic annihilation (creation) operators at site i , $n_i = b_i^\dagger b_i$, r_{ij} is the distance between sites i and j , r_c is the cutoff radius of interactions, and t is the tunneling rate on a lattice of spacing $a = 1$. Interactions such that in Eq. (1) have been proposed [7–9], and recently observed [10, 11], in experiments using laser-dressed Rydberg atoms in optical lattices.

The basic mechanism for Bose metal behaviour in the aforementioned models is rooted in the emergence at

strong coupling ($V \gg t$) of degrees of freedom that are unrelated to individual particles. These are clusters of particles and holes that are effectively bound by repulsive interactions at high enough density, where cluster formation is a generic feature of interaction potentials with negative Fourier components [12] on a lattice [13]. The corresponding classical ground state displays an extensive degeneracy resulting from the exponentially large number of ways in which the cluster can be arranged. This behaviour is similar to that observed in Refs. [13, 14] for the corresponding one-dimensional case, where the quantum dynamics within the low-energy degenerate manifold gives rise to a gapless phase of matter at strong coupling that is not directly captured by Luttinger liquid theory, as evidenced by a deformation of the Bose surface with increasing interaction strength. The one-dimensional results exemplify that soft-shoulder interactions can indeed stabilize phases of matter with (i) no broken symmetries and (ii) off-diagonal quasi-long-range order. In addition, they provide a robust, and essentially classical, mechanism to (iii) decouple the degrees of freedom from the individual particles. These observations constitute an ideal starting point for the investigation of possible quantum spin liquid behavior in the corresponding two-dimensional case, which is the purpose of this work.

In order to demonstrate that quantum fluctuations can induce a Bose-metal phase, we first perform an analysis of the classical problem that demonstrates the formation of a ground-state manifold with extensive exponential degeneracy as a result of cluster formation. This classical solution is equivalent to the problem of a tiling of a surface with tiles of different shapes, the latter being determined by the combined effects of finite-range potentials,

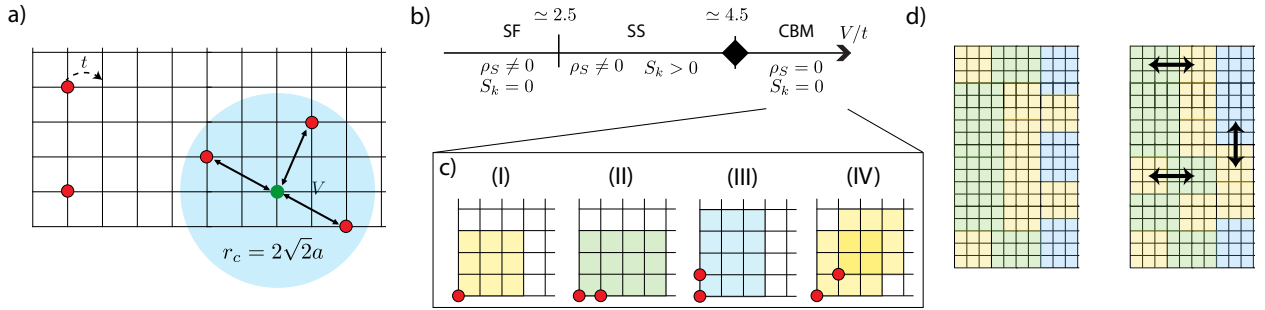


FIG. 1. *Model Hamiltonian and phase diagram.* (a) In model Eq. (1), particles are confined to a square lattice with spacing a , and interact via a soft-shoulder potential of range $r_c = 2\sqrt{2}a$ (blue area for the green particle). t is the kinetic energy. (b) Sketch of the phase diagram as a function of V/t for density $\rho = 5/36$, including superfluid (SF), supersolid (SS), and Cluster Bose Metal (CBM) phases. The observables superfluid density ρ_s , static structure factor $S(\mathbf{k})$, and the momentum distribution $n(k)$ are utilised to distinguish the various phases. The black diamond represents the transition point, discussed elsewhere [22]. (c) In the CBM, the effective dynamics is determined by clusters of type (I-III), which locally minimize the potential energy, while other shapes [e.g., (IV)] are energetically unfavored. (d) Examples of possible cluster moves within the cluster phase.

lattice geometry and density.

We then analyse the quantum mechanical problem by utilising large-scale Monte-Carlo simulations. All results are obtained and verified with two different numerically exact quantum Monte-Carlo techniques. We show that the single particle Green function decays algebraically as a function of distance in the absence of any superfluidity or even crystalline order. This feature and a clear deformation of the Bose surface in the absence of broken symmetries make our system consistent with the expected behaviour of Bose metals [4]. Crucially, the mechanism we propose is remarkably different from the established scenario of gauge theories emergent in quantum dimer models [15], since, as we show below, a direct identification of the lattice Gauss law is here not possible.

We start our discussion by illustrating how an extensive ground state degeneracy is realized in the classical limit of Eq. (1). We are interested here in the regime $2\sqrt{2} < r_c/a < 3$, where each particle tries to establish an avoided region of square geometry with total area $16a^2$ [see Fig. 1(a)]. In this regime, for densities $\rho = 1/9$, the system can arrange into a state with zero energy. However, this is not possible for higher densities, and the ground state shall be constructed as the solution of a tiling problem of three types of clusters, depicted in Fig. 1(c) (I-III). We note that particles now prefer to sit on nearest-neighbors to minimize the potential energy per area, and thus per particle. An exact solution can then be formulated on lattices where the density $1/9 < \rho < 1/6$ can be decomposed into contributions from clusters with total number of particles $N = N_1 + 2 \cdot N_2$ and volume $\mathcal{V} = 9 \cdot N_1 + 12 \cdot N_2$, with N_1 and N_2 the number of clusters made of one (I) or two particles (II-III), respectively. Fixing the ratio $N_2/N_1 = \kappa$, the density reads: $\rho = (1 + 2 \cdot \kappa)/(9 + 12 \cdot \kappa)$. The resulting ground state consists of all permutations of blocks of types I and II-III, and, similar to the one dimensional

case [13, 14], it displays an exponentially extensive degeneracy. As an example, in the following we focus on the case $\rho = 5/36$, for which, for lattice sizes multiple of four, $N_1/\mathcal{V} = 1/18$ and $N_2/\mathcal{V} = 1/24$ [16], and the classical energy of the configurations is $E/\mathcal{V} = V \cdot N_2/\mathcal{V} = V/24$. The demonstration of a robust classical mechanism for engineering this extensive degeneracy is the first result of this work. In the following, we focus on the quantum case with $t > 0$, where quantum fluctuations induce an effective dynamics on top of the classical ground state manifold with a characteristic energy scale $\propto t^2/V$ [see Fig. 1(d)].

The quantum phase diagram of Eq. (1) is investigated by means of large-scale Path Integral Quantum Monte Carlo simulations using two different numerical approaches i.e., the stochastic Green's function algorithm [17] and the worm algorithm [18]. These two methods are largely complementary, as they work in the canonical and grand-canonical ensembles, respectively, and constitute the state-of-the-art techniques to investigate quantum bosonic models on a lattice. Here, we consider sizes up to $L \times L = 48 \times 48$ lattice sites and temperatures as low as $k_B T = t/20$, where k_B is the Boltzmann's constant (set to 1 in the following). We perform careful annealing as well as, for given sets of system parameters, run independent simulations to avoid possible effects of metastability due to the large low-energy degeneracy discussed above. We obtain estimates of the superfluid density $\rho_s = \langle (W_x^2 + W_y^2) \rangle / (4\beta)$, the static structure factor $S(\mathbf{k}) = \sum_{i,j} \exp[-i\mathbf{k} \cdot (\mathbf{r}_i - \mathbf{r}_j)] \langle n_i n_j \rangle / L^4$ and the Green function $G(\mathbf{r}) = \sum_i \langle b_i b_{i+\mathbf{r}}^\dagger \rangle / L^2$. Here, \mathbf{k} is a generic lattice wave vector, W_i is the winding number in the i -th direction, $\beta = 1/T$ and $\langle \dots \rangle$ stands for statistical average. The results for the phase diagram are summarised in Fig. 1(b). By increasing the interaction strength V/t , the following succession of phases is obtained: a su-

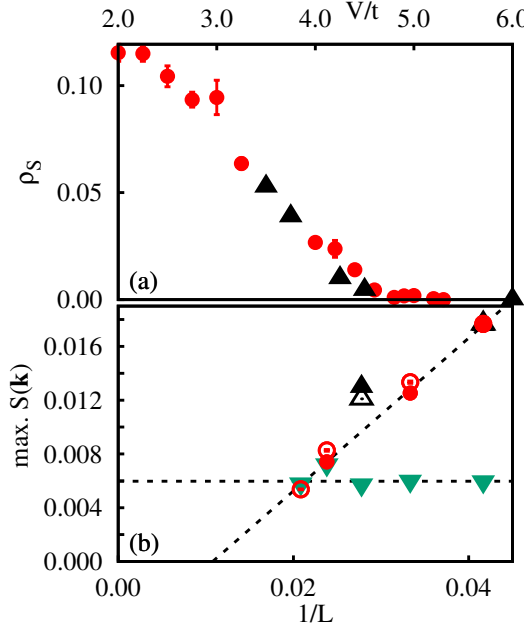


FIG. 2. *Order parameters.* (a) Superfluid density ρ_s as a function of V/t , for $\beta t = 20$ and $L = 36$. In panels (a) and (b), dots and triangles correspond to data obtained with the stochastic Green function and worm algorithms, respectively. (b) Maximal value of the static structure factor $S(\mathbf{k})$ as a function of $1/L$. Green down triangles: $V/t = 4$. Red dots and black up triangles: $V/t = 6$. Full and empty symbols denote $\beta t = 20$ and 4, respectively. Dashed lines are guides to the eye.

perfluid, a stripe supersolid and a cluster Bose metal (CBM). The first two phases are well described in literature: The superfluid [$V/t \lesssim 2.5$] and supersolid phases [$2.5 \lesssim V/t \lesssim 4.5$] are lattice analogs of the corresponding phases in free space [7, 8, 19], characterised by a finite value of the superfluid density ρ_s . We find that due to the presence of the lattice, however, the crystalline order in the supersolid phase, signalled by a small but finite value of the static structure factor in the thermodynamic limit, has a stripe-like character instead of the triangular one observed in free space. Example results for the behaviour of the order parameters ρ_s and $S(\mathbf{k})$ are shown in Fig. 2. In particular, Fig. 2(a) shows the dependence of ρ_s on V/t for $L = 36$ and $\beta t = 20$. Here ρ_s is shown to decrease monotonically from a constant finite value for $V/t \lesssim 2.5$ to zero for $V/t \gtrsim 4.5$. Panel (b) shows that $S(\mathbf{k})$ has a finite value that is size-independent for $V/t = 4$, signalling crystalline order consistent with supersolid behaviour (green down triangles). For $V/t = 6$ (black up triangles and red dots), however, $S(\mathbf{k})$ vanishes in the thermodynamic limit. Interestingly, the values of $S(\mathbf{k})$ for each size are essentially the same at $\beta t = 20$ and 4 (full and empty symbols, respectively). This same behaviour is obtained for other values of the interaction strength $V/t \gtrsim 4.5$. The disappearance of diagonal long

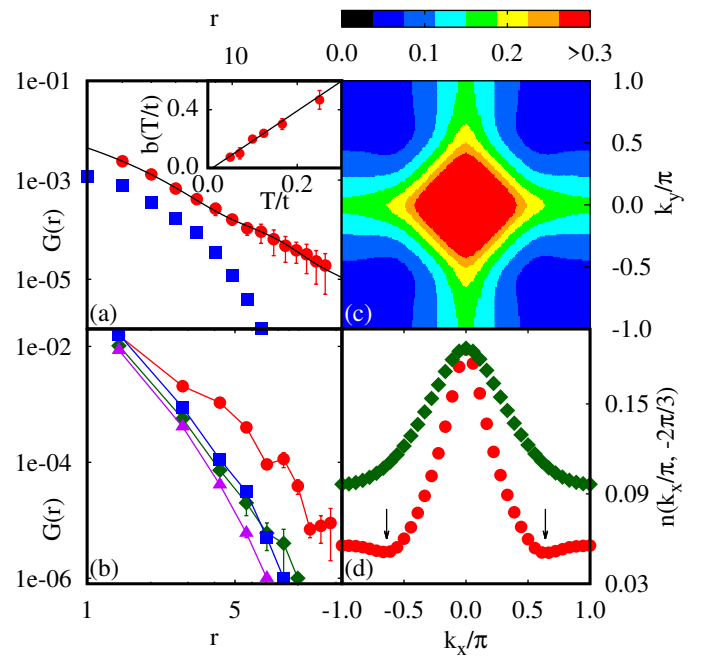


FIG. 3. *Green function and momentum distribution in the CBM phase.* (a) Green function $G(|\mathbf{r}|)$ averaged over the x and y directions *vs* distance r for $V/t = 6$, $L = 36$, $\beta t = 20$ and densities $\rho = 5/36$ (red circles) and $\rho = 7/36$ (blue squares). The black continuous line is a fit to the data using the function $\tilde{G}(r)$ [see Eq. (2) and text] and parameters $a = 0.376 \pm 0.025$, $b = 0.074 \pm 0.016$, $k = 0.407 \pm 0.009$ and $\eta = 0.997 \pm 0.095$. Inset: exponent $b(T)$ of function $\tilde{G}(r)$ *vs* temperature T for $\rho = 5/36$ extracted from fits to numerical data for $G(r)$ at the corresponding temperatures (not shown). The black line is a linear fit. (b) Green function $G(\mathbf{r})$ along the direction $\pi/4$ for $V/t = 6$, $\beta t = 20$, $L = 36$ and densities $\rho = 5/36$ (red circles), $\rho = 6/36$ (green rhombi), $\rho = 7/36$ (blue squares) and $\rho = 8/36$ (purple triangles). (c) Contour plot of the momentum distribution $n(\mathbf{k})$ for the case with $\rho = 5/36$ in panel (a). Points in the red region have $n(\mathbf{k}) > 0.30$. (d) Section of $n(\mathbf{k})$ with $k_y = -2\pi/3$ for $\rho = 5/36$ (red) and $\rho = 6/36$ (green).

range order and superfluidity for $V/t \gtrsim 4.5$ is a first sign of Bose-metal behaviour in the strong-coupling regime with $V/t \gg 1$. In the following we focus on characterising this strong-coupling regime, while the nature of the phase transition around $V/t \simeq 4.5$ will be discussed elsewhere [22].

Surprisingly, we find that correlation functions such as the Green function $G(\mathbf{r})$ decay *algebraically* within the strong-coupling phase, indicating the presence of off-diagonal quasi-long-range order in the absence of a finite ρ_s at sufficiently low temperature for $V/t \gtrsim 4.5$. In addition, the Green function is found to oscillate as a function of distance. An example of this behaviour for the $G(|\mathbf{r}|)$ averaged over the x and y directions is shown in Fig. 3(a) for the case $L = 36$ and $\beta t = 20$. In panel (a), the asymptotic algebraic decay is clearly distinguishable for

the density $\rho = 5/36$ (red dots) that corresponds to the classical tiling solution discussed above, in contrast to the density $\rho = 7/36$ (blue squares) that shows an exponential decay. The oscillations of the Green's function with distance are clearly evidenced by plotting $G(\mathbf{r})$ along specific directions. Panel (b) shows an example for a chosen angle of $\pi/4$, where the oscillations in $G(\mathbf{r})$ are clearly visible for $\rho = 5/36$ (red dots), in contrast to the behaviour for different densities: For densities not supporting a classical cluster solution, $\rho = 6/36, 7/36, 8/36$, the Green's function is found to decay exponentially signalling the loss of long-range phase coherence. This identifies clustering as the backbone ingredient for the stability of the cluster liquid phase.

The oscillations of $G(\mathbf{r})$ result in a deformation of the Bose surface, as depicted in Fig. 3(c). The latter is a contour plot of the momentum distribution $n(\mathbf{k})$ for the same parameters of panel (a), which displays pinch points around $(k_x, k_y) = (\pi/2, \pi/2)$. The pinch points are even more visible in panel (d) for a specific choice of $n(k_x, k_y = -2\pi/3)$ (red dots). Again this feature is absent for different densities, where the cluster structure corresponding to the solution of the classical tiling problem is absent (green rhombi for $\rho = 6/36$). The algebraic decay of the correlation functions together with the observed deformation of the Bose surface shown above in the absence of superfluidity or crystalline order demonstrate the existence of a spin-liquid-type phase at strong coupling, which we term Cluster Bose Metal. This is the central result of this work.

The demonstration of a Bose metal in the simple square extended Hubbard model is a surprising result. In the remainder of this work, we attempt a qualitative interpretation. We start by noting that while the bosonic system above cannot have nodes in the underlying ground-state wave-function, and thus there can be no singularities in $n(\mathbf{k})$, the structure of the momentum distribution found in Fig. 3 closely resembles the open Fermi surface of d-wave Bose liquids as proposed in Ref. [4]. The latter correspond to a U(1) gauge theory coupled to spin-1/2 fermions. In that theory, the long-distance behavior of the Green's function at zero temperature has the expected form

$$G^0(\mathbf{r}) = a \left[\frac{\cos[(\mathbf{k}_1 - \mathbf{k}_2) \cdot \mathbf{r}]}{|\mathbf{r}|^{4-\eta}} + \frac{\cos[(\mathbf{k}_1 + \mathbf{k}_2) \cdot \mathbf{r} - 3\pi/2]}{|\mathbf{r}|^4} \right], \quad (2)$$

with a and η constants, and \mathbf{k}_1 and \mathbf{k}_2 the Fermi momenta of the fermion fields. While an exact mapping between U(1) gauge theories and our cluster models, akin to the ones proposed for quantum dimer models [20], is not possible in two dimensions, due to the exotic form of the cluster constraints which do not lend themselves to an interpretation in term of Gauss laws, we note that for the one-dimensional case [14] it is indeed possible to relate analytically the cluster dynamics to the Schwinger

model [QED in (1+1)-dimensions] in the weak coupling limit [23], where the role of the fermions is played by clusters of two particles, while clusters of single particles correspond to the (bare) vacuum. Based on this 1D behavior of the cluster model, it is suggestive to attempt to describe the low-energy dynamics of the 2D model under consideration as a U(1) gauge theory coupled to a pair of emergent matter fields, one describing the dynamics of clusters of type (II), and one of type (III) in Fig. 1. This identification immediately implies that the corresponding (angle averaged) Fermi momenta of the two emergent modes should be equal in our cluster Bose metals, and similar to the ones which can be obtained in the classical limit, $k_F \simeq \pi/4 = k_{cl}$. Incidentally, emergent Fermi fields with equal Fermi momenta would also ensure positivity of the Green's function.

We test the qualitative picture above by fitting the function $\tilde{G}(r) = G^0(r) \exp(-br)$ to the numerical quantum Monte-Carlo data for the Green's function in Fig. 3(a) (solid line), where $G^0(r)$ has the form of Eq. (2) with $k_1 = k_2 = k_F$, and the exponential factor has been inserted to take into account that we always have a finite T in our Path-Integral quantum Monte-Carlo simulations (here, $\beta t = 20$). The figure shows a good agreement with the numerical data for $\eta = 0.997 \pm 0.008$ and $b = 0.074 \pm 0.016$, while $k = 0.407 \pm 0.001$. Similar agreement is found for different values of V/t in the CBM phase. In the Inset of Fig. 2(a) we plot the extracted exponent b as a function of T obtained by fitting $\tilde{G}(r)$ for different temperatures. The extrapolated value of $b(T = 0)$ is consistent with zero, which further corroborates the existence of off-diagonal quasi-long-range order in the CBM phase.

In summary, in this work we have demonstrated a novel mechanism for the realisation of Bose metal behaviour in the extended Hubbard model with two-particle interactions. The simplicity of the model discussed here paves the way to the observation of Bose metal behaviour in various microscopic systems, including laser-dressed Rydberg atoms in optical lattices [7–9], where the realization of soft-shoulder potentials has recently been reported [10, 11]. Extending this work to fermionic systems with variable interaction range supporting clusters could shed light on the microscopic mechanism of non-Fermi liquid behaviour in two-dimensional extended Fermi-Hubbard models.

We acknowledge useful discussion with A. Kuklov, W. Lechner, M. Mattioli, and S. Wessel. Work in Strasbourg was supported by the ERC St-Grant ColDSIM (No. 307688), with additional funding from Rysq and ANR-FWF grant BLUESHIELD. Work in Innsbruck was supported in part by the ERC Synergy Grant UQUAM, SIQS, and the SFB FoQuS (FWF Project No. F4016-N23). T. Y. was also supported by the National Natural Science Foundation of China (No. 11504067).

[1] Feigelman, M. V. Geshkenbein, V. B. Ioffe, & L. B. Larkin, A. I. Two-dimensional Bose liquid with strong gauge-field interaction. *Phys. Rev. B* **48**, 16641 (1993).

[2] Phillips, P. & Dalidovich, D. The elusive Bose Metal. *Science* **302**, 243 (2003).

[3] Tsien, A. W. Hunt, B. Kim, Y. D. Yuan, Z. J. Jia, S. Cava, R. J. Hone, J. Kim, P. Dean, C. R. & Pasupathy, A. N. Nature of the quantum metal in a two-dimensional crystalline superconductor. *Nature Physics* **12**, 208-212 (2016).

[4] Motrunich, O. I. & Fisher, M. P. A. d-wave correlated critical Bose liquids in two dimensions. *Phys. Rev. B* **75**, 235116 (2007).

[5] Jiang, H.-C. Block, M. S. Mishmash, R. V. Garrison, J. R. Sheng, D. N. Motrunich, O. I. & Fisher, M. P. A. Non-Fermi-liquid d-wave metal phase of strongly interacting electrons. *Nature* **493**, 39 (2013).

[6] Block, M. S. Sheng, D. N. Motrunich O. I. & Fisher, M. P. A. Spin Bose-Metal and Valence Bond Solid Phases in a Spin-1/2 Model with Ring Exchanges on a Four-Leg Triangular Ladder. *Phys. Rev. Lett.* **106**, 157202 (2011).

[7] Henkel, N. Nath, R. & Pohl, T. Three-dimensional Roton-Excitations and Supersolid formation in Rydberg-excited Bose-Einstein Condensates. *Phys. Rev. Lett.* **104**, 195302 (2010).

[8] Cinti, F. Jain, P. Boninsegni, M. Micheli, A. Zoller, P. & Pupillo, G. Supersolid droplet crystal in a dipole-blockaded gas. *Phys. Rev. Lett.* **105**, 135301 (2010).

[9] Honer, J. Weimer, H. Pfau, T. & Büchler, H. P. Collective many-body interaction in Rydberg dressed atoms. *Phys. Rev. Lett.* **105**, 160404 (2010).

[10] Jau, Y. Y. Hankin, A. M. Keating, T. Deutsch, I. H. & Biedermann, G. W. Entangling atomic spins with a Rydberg-dressed spin-flip blockade. *Nature Physics* **12**, 71-74 (2016).

[11] Zeiher, J. van Bijnen, R. Schauss, P. Hild, S. Choi, J.-Y. Pohl, T. Bloch, I. & Gross, C. Many-body interferometry of a Rydberg-dressed spin lattice. *Nature Physics* **12**, 1095-1099 (2016).

[12] Mladek, B. M. Gottwald, D. Kahl, G. Neumann, M. & Likos, C. N. Formation of Polymorphic Cluster Phases for a Class of Models of Purely Repulsive Soft Spheres. *Phys. Rev. Lett.* **96**, 045701 (2006).

[13] Mattioli, M. Dalmonte, M. Lechner, W. & Pupillo, G. Cluster Luttinger Liquids of Rydberg-Dressed Atoms in Optical Lattices. *Phys. Rev. Lett.* **111**, 165302 (2013).

[14] Dalmonte, M. Lechner, W. Cai, Z. Mattioli, M. Läuchli, A. M. & Pupillo, G. Cluster Luttinger liquids and emergent supersymmetric conformal critical points in the one-dimensional soft-shoulder Hubbard model. *Phys. Rev. B* **92**, 045106 (2015).

[15] Zhou, Y. Kanoda, K. & Ng, T.-K. Quantum Spin Liquid States. *Rev. Mod. Phys.* **89**, 025003 (2017).

[16] We note that for some of the system sizes considered here, where $\text{mod}_4 L = 2$, there are multiple cluster configurations attainable with different densities: in this case, we sample both cases in the QMC simulations.

[17] Rousseau, V. Stochastic Green function algorithm. *Phys. Rev. E* **77**, 056705 (2008).

[18] Prokof'ev, N. V. Svistunov, B. & Tupitsyn, I. Exact, Complete, and Universal Continuous-Time Worldline Monte Carlo Approach to the Statistics of Discrete Quantum Systems. *JETP* **87**, 310 (1998).

[19] Cinti, F. Macrì, T. Lechner, W. Pupillo, G. & Pohl, T. Defect-induced supersolidity with soft-core bosons. *Nature Comm.* **5**, 3235 (2014).

[20] Lacroix, C. Mendels, P. & Mila, F. *Introduction to Frustrated Magnetism: Materials, Experiments, Theory*, (Springer, Heidelberg, 2011).

[21] $L=24$ it is the smallest size available where the cluster can re-arrange in parallel wires.

[22] Ying T. *et al.*, in preparation (2017).

[23] Schwinger, J. Gauge Invariance and Mass. II. *Phys. Rev.* **128**, 2425 (1962).